

UC Riverside

UC Riverside Previously Published Works

Title

Green fluorescent protein as an indicator of cryoinjury in tissues.

Permalink

<https://escholarship.org/uc/item/9pt9k4wb>

Journal

Annals of biomedical engineering, 41(12)

ISSN

0090-6964

Authors

Slade, Adam B
Martínez-Suástegui, Lorenzo A
Vié, Florian
et al.

Publication Date

2013-12-01

DOI

10.1007/s10439-013-0874-7

Peer reviewed

Green Fluorescent Protein as an Indicator of Cryoinjury in Tissues

Adam B. Slade, Lorenzo A. Martínez-Suástegui, Florian Vié & Guillermo Aguilar

Annals of Biomedical Engineering
The Journal of the Biomedical
Engineering Society

ISSN 0090-6964
Volume 41
Number 12

Ann Biomed Eng (2013) 41:2676-2686
DOI 10.1007/s10439-013-0874-7



Your article is protected by copyright and all rights are held exclusively by Biomedical Engineering Society. This e-offprint is for personal use only and shall not be self-archived in electronic repositories. If you wish to self-archive your article, please use the accepted manuscript version for posting on your own website. You may further deposit the accepted manuscript version in any repository, provided it is only made publicly available 12 months after official publication or later and provided acknowledgement is given to the original source of publication and a link is inserted to the published article on Springer's website. The link must be accompanied by the following text: "The final publication is available at link.springer.com".

Green Fluorescent Protein as an Indicator of Cryoinjury in Tissues

ADAM B. SLADE,¹ LORENZO A. MARTÍNEZ-SUÁSTEGUI,² FLORIAN VIÉ,³ and GUILLERMO AGUILAR^{1,4}

¹Department of Mechanical Engineering, University of California Riverside, Riverside, CA 92521, USA; ²ESIME Azcapotzalco, Instituto Politécnico Nacional, Avenida de las Granjas No. 682, Colonia Santa Catarina, Delegación Azcapotzalco, Mexico, Distrito Federal 02250, Mexico; ³Department of Nuclear Engineering, National Graduate School of Engineering and Research Center of Caen (ENSICAEN), 6, Boulevard du Maréchal Juin CS 45053, 14050 Caen Cedex 04, France; and ⁴Department of Bioengineering, University of California Riverside, Riverside, CA 92521, USA

(Received 25 March 2013; accepted 18 July 2013; published online 30 July 2013)

Associate Editor James Tunnell oversaw the review of this article.

Abstract—The fluorescence intensity of Green Fluorescent Protein (GFP) has previously been demonstrated to be an accurate indicator of cellular viability following cryoinsult in individual GFP-transfected cells. In an attempt to ascertain whether GFP fluorescence intensity may also be used as a viability indicator following cryogenic insults in whole tissues, this study examines the transient fluorescence intensity of GFP-transfected mouse hepatic tissue *ex vivo* following cryoinsult. The observed trends are compared with diffusion-based models. It was observed that the fluorescence intensity of the exposed tissues exhibited slow exponential decay, while the solution in which the tissues were placed inversely gained fluorescence. This slow decay (~3 h) is in contrast to the rapidly diminished fluorescence intensity (seconds) seen in GFP-cell cultures following cryoinsult. These trends suggest that mass diffusion of GFP in the interstitial space, and ultimately into the surrounding medium, is the primary mechanism which determines the fluorescence loss in cryoinjured tissues. These results suggest GFP-transfected tissues may be effectively used as indicators of cryoinjury, and hence viability, following hypothermal insult provided that a sufficiently long incubation is held before observation. It was found that a meaningful observation (15% reduction in fluorescence) could be made three hours subsequent to cryoinjury for the tissues used in this study.

Keywords—Cryoinsult, Cryosurgery, Diffusion, Hyperthermia, Hypothermia, Fluorescence, Laser, Viability.

INTRODUCTION

Cryosurgery—the precise application of cryogenic temperatures—is often used to selectively devitalize

cancerous or precancerous tumors, arresting its propagation through healthy tissue. These low temperatures serve to rupture the plasma cell membranes, or to dehydrate the cells as to render their vitality compromised. To determine the success of a cryosurgical protocol, it is of critical importance that the tissues cryogenically treated, as well as the surrounding tissues, be evaluated for their viability. Current viability protocols require the tissue to be excised from the treatment site and examined *in vitro*.^{9,17} These procedures are invasive and provide only information traceable to the moment in time when the biopsy was obtained. Non-invasive viability assays can be utilized to determine cellular viability, but require the addition of chemical tracers (which are often toxic or phototoxic) to the living tissue.¹³ While viability can be determined optically without tracers, this is done on a cell-to-cell basis,⁴ and assessing the viability of a whole tissue would not be feasible using those methods.

Green Fluorescent Protein (GFP) is a protein derived from jellyfish which can be and has been transposed into the genome of a myriad of organisms. It has the effect of causing transfected tissues to fluoresce green when illuminated with blue light, and has recently found use as a viability assay in cell cultures.³ GFP has the advantage over other viability assays in that it can be examined *in situ*, and can also be continuously monitored to examine the transient viability of the cells using optical imaging, thereby making it an ideal indicator of animal tissue viability in research protocols.

The GFP molecule has a tight cylindrical barrel shape, which protects it from a moderate range of thermal trauma,¹⁸ however, at sufficiently elevated temperatures (> 50 °C) its structure becomes “unwound”,

Address correspondence to Guillermo Aguilar, Department of Mechanical Engineering, University of California Riverside, Riverside, CA 92521, USA. Electronic mail: aslade@engr.ucr.edu, lamartinez@ipn.mx, gaguilar@engr.ucr.edu

it is compromised (irreversibly denatured) and exhibits loss of fluorescence.¹ In contrast, after exposing GFP cells to cryogenic temperatures (liquid nitrogen: -196°C), they appear to remain stable and exhibit only a slightly reduced quantum fluorescent yield.^{6,10} Therefore, while GFP-transfected tissue exhibits immediate loss of fluorescence following hyperthermal insults, hypothermal insults have no such immediate effect. In fact, in preliminary trials using GFP as an indicator of viability in whole tissues, it was observed that there is a delayed response on the order of several hours to changes in fluorescence in cryoinjured tissues.⁷ In addition to temperature, GFP fluorescence also exhibits sensitivity to the pH of its environment. However, while the fluorescent yield drops off in very acidic or basic solutions, there is a relatively wide range of pH values for which fluorescence is stable.^{1,2}

This tissue-based studies are in contrast with single cell studies, which report immediate fluorescence change following both hyperthermal and hypothermal insults.³ Furthermore, in the latter study focused on cell cultures, it was implied that the loss of cell fluorescence following cryoinsult corresponds with the physical loss of GFP from inside a GFP-transfected cell, however, it was not demonstrated conclusively that this was the only driver contributing to fluorescence loss, nor the transient fluorescence intensity decay following cryoinsult was reported. This opened an interesting quandary as it is also plausible, in principle, that the viability of cells transfected with the GFP vector is also linked to the relative amount of expressed fluorescence, with the most brightly fluorescing cells being viable, and apoptotic or necrotic cells exhibiting diminished fluorescence.¹⁴

This work aims to observe the time-dependent nature of GFP fluorescence to identify the mechanism that drives fluorescence loss after hypothermal insults. For this purpose, it is hypothesized that there is a relationship between the fluorescence of a GFP-transfected tissue post-cryogenic insult and the rate of diffusion of GFP from the compromised tissue into the surrounding tissue or incubation medium. To prove this hypothesis, the known phenomena which affect the fluorescence of GFP (i.e., pH, temperature, excitation light intensity and excitation duration) are maintained within ranges known not to affect GFP fluorescence yield. The transient fluorescence of a cryogenically-treated tissue is then compared to mass diffusion models to determine its correlation (or lack thereof). Finally, the fluorescence of the incubation medium is compared to the total fluorescence of the tissue to establish a balance between tissue and incubation medium fluorescence gain/loss.

MATERIALS AND METHODS

GFP Tissue Harvesting and Sample Preparation

The strain of GFP used in this study is the enhanced GFP which has an electromagnetic radiation absorption (excitation) peak at 488 nm (blue light), and an emission peak at 509 nm (green light) (Fig. 1).

According to protocols A-20080013 and A-20080019, approved by the UCR Institutional Animal Care and Use Committee (IACUC), all GFP-transfected tissues used in this study were harvested from the hepatic tissue of GFP-transfected mice. This specific tissue was chosen due to its large size, ease of extraction and similar thermal properties compared to other available organs.⁷ The specific GFP vector transcription used, C57BL/6-tg(UBC-GFP)30Scha/J, universally expresses GFP in mouse tissue under the human ubiquitin C (UBC) promoter.¹² This strain of GFP was used as it has relatively little overlap in its excitation and emission curves (only between 470 and 530 nm), thus the excitation source light may be completely isolated from captured emission light from the tissue to eliminate all crossover illumination.

After the mice were euthanized *via* CO_2 asphyxiation, the liver was excised and cut into squares of 6×6 mm, and left at its native thickness of approximately (but not uniformly, exactly) 4.4 mm. The thickness of the samples varied spatially by up to approximately 20% from their mean value, as determined visually. These dimensions were chosen as they were similar in size to previous GFP-tissue studies

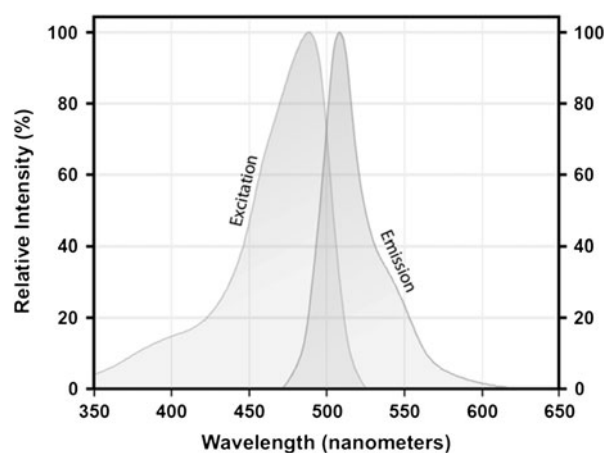


FIGURE 1. GFP excitation and emission curves. The curves show the relative strength of excitation and emission wavelengths for GFP. The overlap of the two curves indicates the wavelengths at which GFP both absorbs and emits light. To eliminate crossover, a low-pass filter at 500 nm is used for the illumination, and a band-pass filter with lower-limit at 510 nm is used for the fluorescence. Figure adapted from Nikon MicroscopyU.

performed in this laboratory.⁷ Following excision and trimming, all samples were immersed together in 50 mL of isotonic Phosphate Buffered Saline (PBS) solution (pH 7.4) to prevent tissue damage due to cellular dehydration. The PBS also served to maintain the pH level without significant change. Samples remained in this holding vessel for approximately 2 min to allow for experimental preparation time.

Control samples were removed from the holding vessel and placed in an isolated 34 mm cylindrical vessel and covered with 5 mL of fresh PBS. The samples slated for cryoinjury were removed from the holding vessel, and one side was exposed for one minute to a cryoprobe cooled by circulating liquid nitrogen at -196°C . This exposure time was long enough to ensure that the entire sample was uniformly cooled to a temperature of -150°C or lower as measured by a 0.2 mm-diameter hypodermic thermocouple inserted into the sample's center, ensuring complete cellular necrosis. Following the cryoprobe contact, cryoinjured samples were placed in fresh PBS (identical to control tissues) at room temperature (23°C), thawing in a few seconds. Nothing was placed over the sample/PBS as to keep the optical path clear. Both the cryoinjured samples and control samples were then isolated from all light to prevent photobleaching. Ten tissue samples were used in the experiments, with five as control tissues (no thermal damage) and the remainder as cryogenically injured tissues (necrotic). In addition, one sample served as an inverse control, where all GFP within the tissue was irreversibly denatured through immersing the sample in water at 100°C for 5 min. Also, a set of four samples were prepared for qualitative visual analysis, consisting of two tissue samples prepared in the same manner as the control/cryogenic treatments described above; one sample cryogenically treated through submersion in liquid nitrogen for 5 min; and one sample boiled in water for 5 min.

Fluorescent Image Acquisition

A custom fluorescence microscope was constructed to measure the fluorescence intensity of the GFP-transfected tissue as a function of time. A brief description of the experimental apparatus is as follows.

When the sample is to be illuminated (fluorescently excited), a mechanical shutter blocking a broadband light source (Fiber Lite[®] MI-150 utilizing an EKE 21 V 150 W halogen projector lamp routed via stock fiber optics) opens (Fig. 2-1), allowing light to proceed through focusing optics and a low-pass excitation filter (Thorlabs, model FES0500). The mechanical shutter is used to limit exposure and thus prevent photobleach of the GFP within the tissue. After the light passes

through the shutter and excitation filter, the light reflects off a dichroic filter (Thorlabs, model DMLP505, Fig. 2-2) whose surface is positioned 45° to the incoming light. This filter selectively transmits or reflects the light (high-pass, low-reflect), further narrowing the bandwidth of excitation light. The reflected light illuminates the tissue at approximately 215 W/m^2 (Fig. 2-3) where it is both in part reflected and absorbed. A portion of the absorbed light excites the GFP within the tissue, which reemits this absorbed light at a longer wavelength. The light which is reemitted in the upwards direction passes through the dichroic filter again at an angle of incidence of 45° (high-pass, low-reflect), followed by a band-pass emission filter (Thorlabs, model FB550-40), that isolates pure GFP fluorescence from reflected illumination light. This isolated fluorescence then passes through the camera's RGB Bayer-pattern filter (designed to record wavelength information) and then is collected by the CCD's (Sony IXC282AQ Super HAD CCD) capacitive bins (Fig. 2-4). Note that the optical setup could be achieved using a modified optical path. For example, the dichroic could be used without the excitation filter to allow for greater light excitation, and the excitation light may include all wavelengths shorter than the pass-wavelength of the excitation filter, if so desired.

The CCD begins photon capture after the mechanical shutter opens. The electronic shutter stays open long enough for the CCD to collect enough light to produce an image, but not beyond the time in which any particular capacitive bin might saturate. After this predetermined length of exposure (directly proportional to the illumination intensity), both the CCD's electronic shutter and the mechanical shutter close. As the entire system is isolated from ambient light, this leaves the sample in complete darkness until the next image is to be acquired, negating the possibility of photobleaching. This computer-controlled system exposes and images a single sample for 5 s once every 3 min. This imaging process was allowed to proceed over the course of several hours, until the tissue fluorescence reached a steady value (6–12 h). All imaging components were permitted to reach their steady state temperature before imaging commenced. Electronic noise inherent in the sensor was averaged out over space and time, that is, the brightness of the image was taken as a regional average (described below), and smoothed among subsequent images.

Data Processing

It was observed that while the samples generally exhibited a decrease in fluorescence over the acquisition period, the PBS in which the samples were placed steadily increased in fluorescence. Both the tissue and

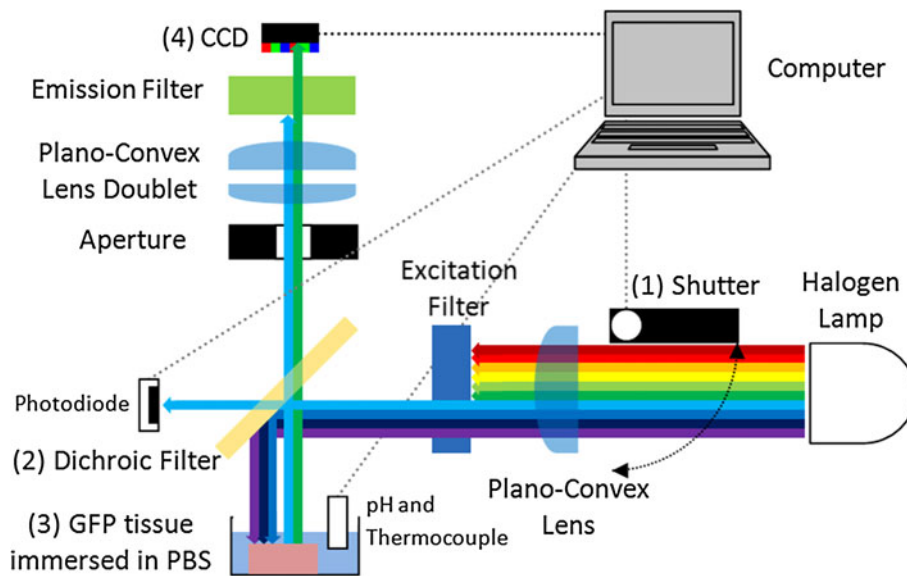


FIGURE 2. Experimental setup for the isolation and collection of GFP fluorescence. The image acquisition is similar to a standard fluorescence microscope, with the distinction that a mechanical shutter is incorporated to inhibit illumination between acquisitions (1), and in that there exists additional transducers which monitor illumination intensity, pH of the tissue's buffer solution, and temperature of the tissue.

PBS fluorescence intensities were measured by acquiring CCD images from two different regions. One region of the image contains the GFP tissue (along with the PBS on top of the tissue) and the other region of interest is to the side of the tissue sample where only PBS was imaged. Each image in the sequence had the same field of view (neither the sample nor imager were moving), and as such a constant subset of the image was determined spatially and applied to all subsequent images. These regions were determined as a maximized region (greater than 80% of the surface area) consisting of only tissue/PBS which provided no overlap between the two regions, as shown in Fig. 3.

Using the known depth of the PBS over the sample (typically 1.3 mm), and the depth of the PBS to the side of the sample (typically 5.7 mm), the fluorescent contribution of the PBS to the tissue region may be subtracted from the fluorescence of the tissue at every time step, resulting in a fluorescent value which is independent of the fluorescence of the surrounding fluid. A separate photodiode recorded the relative illumination intensity of the sample (not wavelength), to ensure consistent sample excitation. Simultaneously, a calibrated type-K thermocouple and calibrated pH probe recorded the temperature and pH of the solution. After each 5 s exposure, the CCD sensor data was sent to a computer where it was compiled into a JPEG image of the sample. The mechanical shutter, image acquisition, pH data recording, photodiode data recording, and data storage were all managed autonomously by a custom LabVIEW® program controlling and getting data from DAQ controllers (National

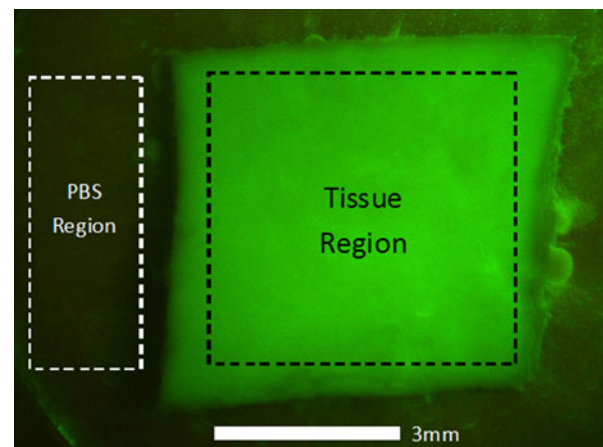


FIGURE 3. Regions of GFP fluorescence image analysis. The “Tissue Region” includes a representative portion of the fluorescing GFP tissue, which is submerged under a layer of PBS. The “PBS Region” includes a representative portion of the incubation PBS, at its full depth.

Instruments). pH and image acquisition were done with a pH sensor (Sensorx® S100C) and a scientific grade camera (Progres® C5), respectively.

After the sequence of images was collected, a custom MATLAB® program analyzed the images from the two stationary regions previously described (tissue, and surrounding PBS) to determine their relative brightness (luminosity), and a correction factor was applied for each image to account for PBS fluorescence affecting the GFP fluorescence. This correction factor was calculated as the relative brightness of the incubation

fluid in the region without tissue, versus the region containing tissue. Furthermore, the data from the photodiode which measured the source light intensity was included for an additional correction factor to rectify any differences in the illumination source.

The basic algorithm of the code included applying the user-defined crops to each image region. The digital-filter was then applied by deleting the blue-channel data from the image. The average spatial luminances of the tissue crop and PBS crop were determined ($AvIm$). Finally the adjusted luminance of the tissue crop ($AdIm$) was obtained by subtraction of the product of the PBS luminance ($AvPBS$) with the determined percentage of PBS depth above the tissue ($PerOver$) (typically 23%) from the average luminance, as shown in the following equation. This was repeated for all images in the sequence, as denoted by the subscript in the equation.

$$AdIm_i = AvIm_i - (PerOver \times AvPBS_i) \quad (1)$$

The output from the MATLAB® image analysis was a matrix giving the raw and corrected tissue luminance for each time step. As it was assumed that GFP fluoresces most brightly in healthy, viable tissue, and that the tissue was most healthy/viable immediately after harvest, the first time step was defined as 100% luminance, and all the data was normalized to that time step. When plotted, this gives the normalized luminance of the tissue versus time. It is also noted that the CCD used was tested for its linear response to illumination levels, to ensure that relative fluorescence levels were directly proportional to their relative CCD values.

The data processing workflow is displayed in Fig. 4.

Finite Element Method (FEM) Modeling

To test the hypothesis of diffusion driving the transient nature of the fluorescence, a finite element method model was created using COMSOL® simulation software. The intention of the model was to examine if transient diffusion was the only physical phenomena responsible for the fluorescent intensity loss of the treated tissue samples. The model involved three-dimensional diffusion in a constant-temperature environment. The governing equation used by the software to evaluate the concentration gradients is based on Fick's second law,

$$\delta_{is} \frac{\partial c}{\partial t} + \nabla \cdot (-D \nabla c) = R \quad (2)$$

where D is the diffusion coefficient for GFP in extracellular-matrix, c is the concentration, R (set to zero) is

the reaction rate, and δ is the time-scale coefficient (set to 1, to reflect actual time). The approximations used assume dilute aqueous solutions and, while the tissue is not an aqueous solution, the fluid content of the tissue is sufficiently high that the approximation is valid. Also note that D for GFP in extracellular-matrix is used in our simulations with a value of $5.6E-11 \text{ m}^2/\text{s}$,^{5,8,15} rather than the diffusion coefficient of GFP in tissue because the simulation is only meant as an order-of-magnitude comparison to the observed loss of fluorescence. Also, while the diffusion coefficient of GFP within the nucleus or cytosol is reported in the literature,¹⁶ the value for GFP in mouse hepatic tissue is not readily available. The size of the simulated tissue matched that of the experimental tissue ($6 \times 6 \times 4.4 \text{ mm}$), and the initial normalized concentration (c) of the sample was set to 1 (100%). All boundary conditions of the model were approximated as a constant concentration (c) of zero, as it is assumed that the surrounding fluid contains no GFP and that the far-removed boundaries remain at that concentration as time progresses. This approximation is valid as a large fluid-to-tissue volume ratio (32:1) was used in the experiments.

As an order of magnitude analysis, the characteristic length of diffusion is useful:

$$L_D = \sqrt{4Dt} \quad (3)$$

where L_D is the diffusion length, D is the diffusion coefficient, and t is a characteristic time. This will be used to explain the differences between single cell GFP viability experiments, and experiments using bulk tissue samples.

As visualization of the COMSOL® model would have to match the optical properties of the experimental tissue, one further, major, approximation was made. The model was assumed to have no diffusion across the bottom surface. In reality there would be no diffusion across the bottom surface, as it was not exposed to the surrounding PBS (in contact with bottom surface of Petri dish), but the top surface was exposed to PBS and would naturally have some diffusion. The depth of PBS above the tissue in the experiments was minimized (approx. 1.3 mm) as to minimize diffusion in that direction, while still keeping the sample hydrated. As the top and bottom surfaces were more-or-less boundaries to diffusion, and seeing that the optical depth of the tissue was unknown, the computational model was collapsed to be a two-dimensional model (with a $6 \times 6 \text{ mm}$ domain) by taking the average fluorescence at all depths (z -direction). All boundary conditions and coefficients used were identical to the 3D model.

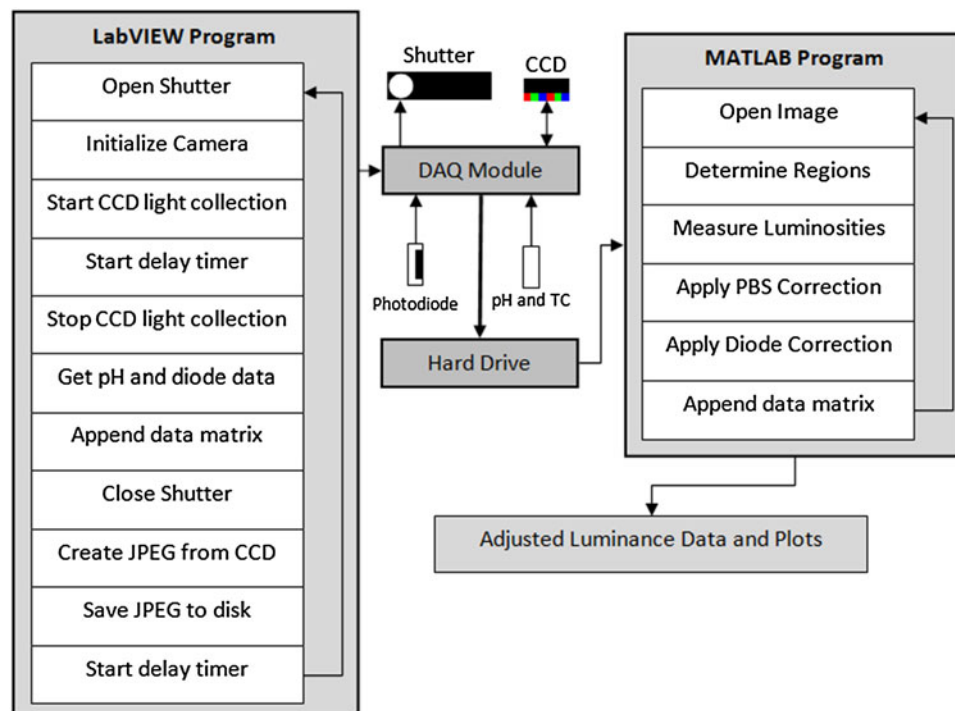


FIGURE 4. Data acquisition and processing flow. The LabVIEW software program instructs the microcontroller to open the optical path shutter. The image is then collected with the camera after the shutter is fully opened. After the image is acquired, the microcontroller also collects data from the photodiode, pH, and TC sensors. The image is organized into a JPEG and sent to the hard drive for storage. A delay timer waits until the next image is to be acquired. Once the data set is completed, custom MATLAB software analyzes the photographs, selecting the image regions (PBS, and tissue), and measures luminosities. The software algorithm then applies correction factors and stores the data in an array and generates plots for further analysis.

GFP Conservation

GFP originally within the tissue was traced from its origin to its final position with the objective to assess the total fluorescence of the entire system (PBS and tissue) for all time steps. In doing so, we aimed at determining if fluorescence intensity loss in the tissue was simply due to diffusion to the surrounding media or if GFP was destroyed or denatured during the procedure. The challenge to this analysis was in that not all fluorescence in the tissue is available to excitation or collection of emission at all times, due to a finite optical penetration depth of the tissue. To examine all fluorescence potential of the tissue, the tissue was dissociated into a suspension of individual cells. This was done with three sets of six tissue samples (18 tissue samples). Each set had three samples dedicated to cryoinjury, and three to control.

In the dissociation procedure, tissue samples were treated with identical thermal insults as in the traditional experiment, however, after incubating in PBS, the sample was removed to a new volume of PBS mixed with collagenase enzyme (to target only collagen peptide bonds, ignoring all other structures (i.e. GFP)¹¹), for extracellular matrix dissolution at a concentration of 100 units/mL. The sample was then permitted to

dissociate over the next 24 h, after which fluorescence of the resulting mixture was examined. As the intention was to examine the average fluorescence of the entire system, cellular integrity did not matter at this point, only GFP integrity. The original incubation PBS was retained for fluorescent analysis, independent of the fluorescence of the dissociated tissue.

As each time-step required an entire tissue sample to be dissociated, samples were only obtained at 1, 3, and 6 h duration, due to limited resources. While this distribution is not ideal for determining the rapid response of GFP fluorescence, it proved to be sufficient in demonstrating the overall trends in fluorescence. Three complete data sets were obtained and averaged using this procedure, for a total of nine samples for the control, and nine for the cryoinjured sample.

RESULTS

Constant pH/Illumination/Temperature

Figure 5 shows the transient pH profile of PBS for a representative experiment. As it has been established that the fluorescent output of GFP is stable within a range of pH from 6 to 10,^{1,2} it is understood that the

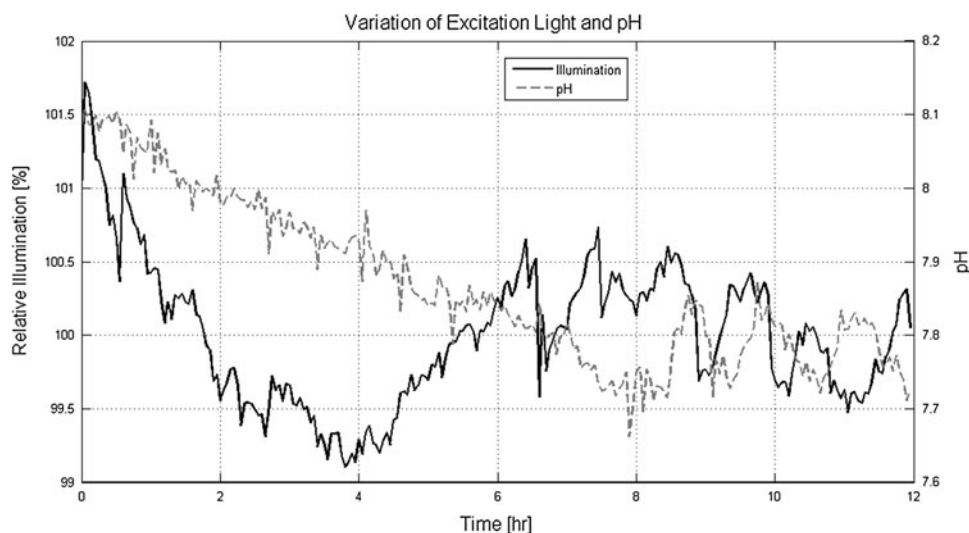


FIGURE 5. Variation of pH and illumination intensity with time. The pH varies between 8.1 and 7.7, which does not significantly alter the fluorescent yield of the tissue. The illumination measured by the photodiode shows some variability, although the intensity never strays further than 1.5% of its average value over the course of 12 h. The data depicted represents a single, representative sample.

observed change in pH will not have any impact of the fluorescent yield of the GFP.

The transient level of excitation light for a representative experiment also shows minimal variability not exceeding 5% of the average value (Fig. 4). However, the fluorescent output of the sample is highly dependent on the illumination intensity, and should be compensated for. To achieve this compensation, each time step was normalized to the measured excitation level for that particular time step.

Finally, the temperature of the system was determined at every time step, and never varied more than ± 2 °C from a mean value of 23 °C. This minimal variability has negligible influence over GFP fluorescence.¹⁰

Optical Results

Figure 6 is subdivided into four quadrants (A–D), all of them showing the fluorescent images of four samples immediately after thermal insults (quadrants A and C) and 20 h. after incubation (quadrants B and D). The top two quadrants (A and B) and bottom two (C and D) represent the same set of four samples, only with crossover between excitation illumination and fluorescent emission (top) and filtered pure fluorescence (bottom). The top left image of each quadrant is the control sample, the top right corresponds to the inverse control and the bottom images to the two cryoinjured samples. The bottom left corresponding to the sample exposed to the cryoprobe for 1 min the bottom right to that immersed in liquid nitrogen for 5 min. These results are only presented here to

provide a conceptual illustration of the results, and these images were not analyzed for numerical data extraction.

Note that the inverse control sample exhibits no green fluorescence, and only reflects back the blue illumination. The other three samples exhibit similar levels of fluorescence. Furthermore, after 20 min of incubation, the control sample still exhibited near-full fluorescence, while the two cryoinjured samples exhibited the same level of diminished fluorescence. The denatured sample, as expected, never exhibited any fluorescence throughout the study.

These images shows that all GFP is denatured immediately in the hyperthermal insult case, as previously reported,¹⁰ and that no fluorescence is immediately lost following hypothermal insults.⁶ They also illustrate that the samples plunged in liquid nitrogen exhibited no measured difference to those frozen using a cryoprobe, indicating that under these conditions both methods completely devitalized the tissue.

Numerical Results

The results of the GFP tissue observation, following cryoinjury, are consistent with what would be expected assuming diffusion of GFP is the mechanism of lost fluorescence. As shown in Fig. 7, the control sample stays at a relatively constant luminance, while the cryoinjured sample loses approximately 15% of its fluorescence over the 6 h of the study. Note that the inverse control (denatured sample) is not plotted here, as it exhibited universally zero fluorescence at all times.

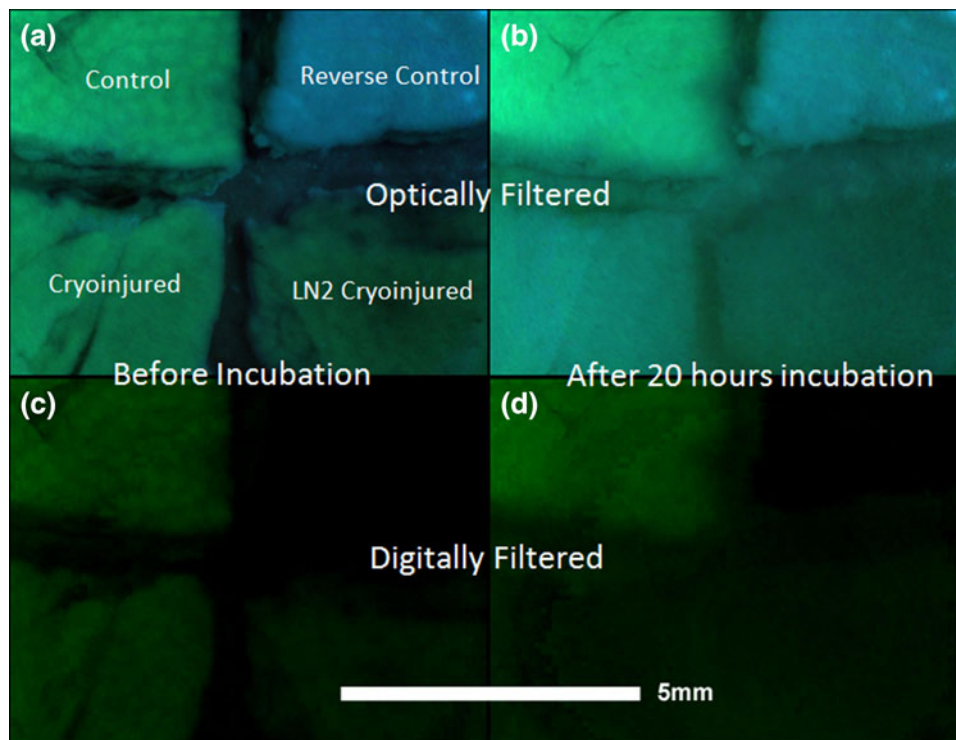


FIGURE 6. GFP fluorescent intensity for control, reverse control and slow-freeze samples, before and after incubation. The top two images have been optically filtered to collect GFP fluorescence, while the bottom two are the same images after additional digital filtering (green channel only). The control shows nearly constant bright fluorescence while the hyperthermal reverse control exhibits constant zero fluorescence and the hypothermal reverse control exhibits constant low fluorescence. Only the low-freeze sample (frozen to -50°C) shows significant change in its fluorescent output, as it starts out at the fluorescence of the control, and ends at the fluorescence of the hypothermal reverse control. Note that these images represent a preliminary data set, which were obtained before the optics were adjusted to exclude all non-fluorescence from the captured images.

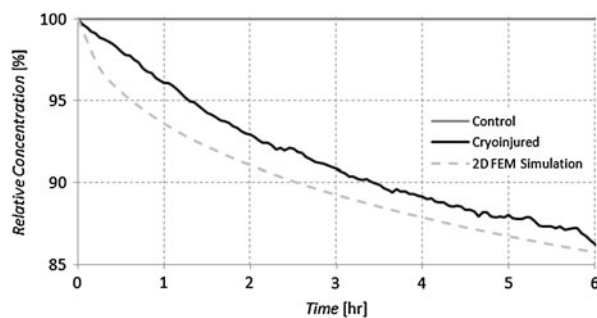


FIGURE 7. GFP transient fluorescence of a representative sample compared to a 2D COMSOL FEM simulation. The experimental data is normalized to the control of the experimental data. A value of $5.6\text{E}-11\text{ m}^2/\text{s}$ was chosen as the diffusion coefficient in the COMSOL model. The concentration at the boundary was set at 80%, to account for “background” fluorescence, or the relative amount that a completely non-viable tissue will fluoresce. Note that the inverse control was measured, but it displayed no fluorescence at any time step, making its value zero (within sensitivity) at all time steps.

The results of the simulation follow the trend of the transient fluorescence of the real tissue. The simulated model does lose fluorescence more rapidly than the tissue, at least, initially.

GFP Conservation

Figure 8 shows the fluorescence of the incubation PBS and tissue dissociation with time. Figure 8a shows that the fluorescence of the incubation PBS for the cryoinjured tissue increases over the first six hours. The increase of GFP in the PBS is due to the loss of GFP from the tissue. It is noted that the control tissue incubated in the PBS also gained some fluorescence over the first 6 h, although it is a smaller fraction of the fluorescence gained by the PBS containing the cryoinjured tissue. Note that the error bars are large for the PBS samples, as they have relatively very little fluorescence when compared to the tissue samples. Error bars represent the standard deviation between samples.

The dissociated tissue curves, shown in Fig. 8b, have a more interesting behavior. It is expected that the fluorescence of the dissociated control tissue remains constant, while that of the cryoinjured tissue decreases (as the fluorescence of the incubation PBS for the cryoinjured tissue correspondingly increases). While this behavior is observed for times in the experiment beyond the three hour mark, both control tissue and cryoinjured tissue start out gaining fluorescence. It suffices to note that relative to the control

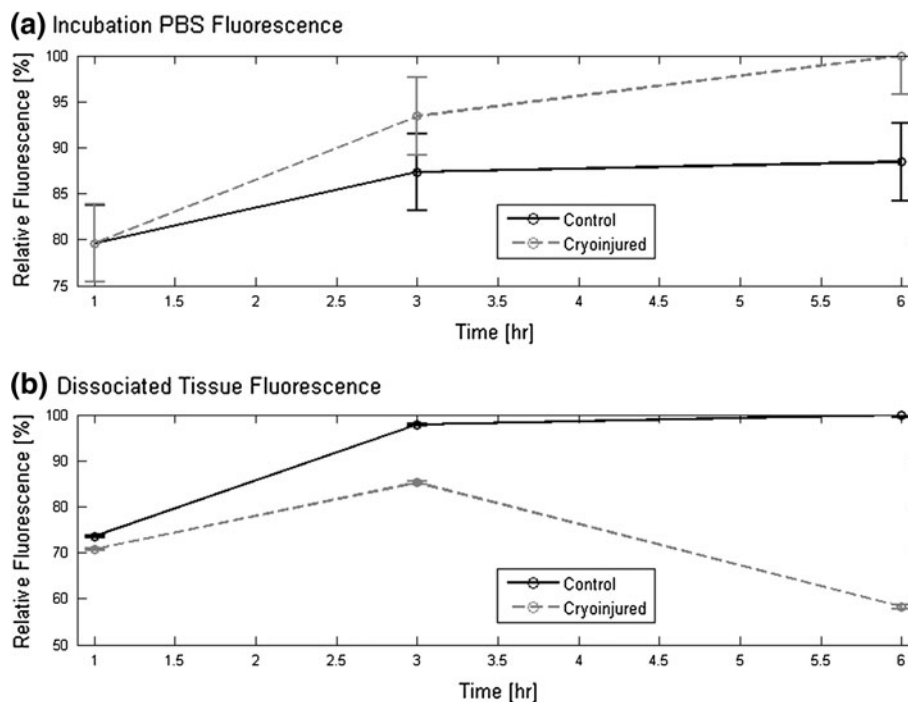


FIGURE 8. Transient fluorescence during dissociation. The fluorescence of the incubation PBS (a) increases with time (during the first 6 h of incubation) for the cryoinjured tissue. The control tissue also increases with time, but to a lesser extent than the cryoinjured tissue incubation PBS. The fluorescence of the dissociated tissue (b) increases during the first portion of incubation for both the cryoinjured and control tissues. Note that after 3 h, the total relative fluorescence of the control sample stabilizes, while the fluorescence of the cryoinjured dissociated tissue begins to decrease (while the fluorescence of the incubation PBS increases).

tissue, the cryoinjured tissue loses fluorescence at every time step, supporting the observed increase in fluorescence of the incubation PBS. Error bars again represent the standard deviation between samples.

DISCUSSION

The results presented in this study are only valid for *ex vivo* cryogenic studies, as it requires both a GFP transfected organism, and relies on long incubation period in an otherwise-static system. It is expected that perfusion in a living system could potentially expedite diffusion results, however this remains untested.

Although the trend of the real tissue follows that of the simulated diffusion model there is some discrepancy between the two. This discrepancy is may come from the assumption of zero GFP-concentration at the system's boundaries. Some error may also be due to the magnitude of the GFP diffusion coefficient, which was based on that occurring in a general extracellular matrix and, thus, not necessarily specific to hepatic tissue. These errors are exacerbated by the unknown optical depth of the tissue, and hence the results are only valid for observation of a trend, which was done here. Note that the fluorescence of the cryoinjured

tissue was only 15% lower than the control tissue after 6 h. In reality, this difference will continue to increase given more incubation time, but the difference becomes readily apparent after this period, and further waiting becomes unnecessary.

The motivation of this study was originally to extend the use of GFP as an indicator of cellular viability, to viability in whole tissues. In the literature supporting the use of GFP as a viability assay for cellular suspensions, there is no mention of any time delay between the cellular cryogenic insult, the observed loss of fluorescence, and cellular viability. In contrast tissue assays exhibit a delayed fluorescent response.

As the driving mechanism of fluorescence loss is diffusion, the difference in single cell and bulk tissue is simply the geometry of the system. A single cell achieves diffusion of GFP very rapidly, while a bulk tissue can require several hours to noticeably exhibit any loss in fluorescent intensity. This difference is illustrated in a comparison of the characteristic time for diffusion between that of single cells (10–50 μm), and that of a bulk (1–100 mm) tissue. A relative comparison between the two length scales can be made through the characteristic time of diffusion equation (Eq. 3).

Solving for t in the equation, it can be demonstrated that the characteristic time of diffusion over the cellular length scale is on the order of several seconds, while the characteristic time of diffusion over the bulk length scale occurs on the order of several hours. Thus, the loss of GFP fluorescence following cryogenic insult may be fully explained by the onset of diffusion of the GFP molecules from the tissue. This result supports the observation that for a single cell the fluorescence loss following cryoinsult occurs over the course of a few seconds,³ while the fluorescence loss from a network of cells (tissue) occurs over the course of a few hours. Further studies may describe the correlation of tissue size determining the characteristic time of diffusion, and the actual observed changes in fluorescence.

Since all factors typically affecting fluorescence yield, such as exposure duration, excitation light intensity, temperature, pH, were kept constant in our study, the observed fluorescence drop can only be attributed to either one of two factors, or both: (1) GFP diffusion from the affected cells into the surrounding medium and/or (2) intracellular effects leading to cell apoptosis and/or necrosis that ultimately yield GFP diminished fluorescence. As the observed drop in fluorescence corresponds with increased fluorescence in the incubation medium, the second condition alone cannot account for the drop in fluorescence, therefore GFP diffusion appears to be if not the only one, at least the major driving force behind transient fluorescence. Furthermore, the trends of the effective diminished fluorescence of the tissue seem to be well represented by Fick's 2nd law (Fig. 6), suggesting again that GFP diffusion is, if not the only mechanism responsible for GFP loss, at least the dominant phenomenon. As such, factors which affect the speed of diffusion (geometry, temperature, surrounding fluid, diffusion coefficient, etc.) will greatly affect the required duration of incubation. For example, for the hepatic tissue used in this study, a rectangular parallelepiped with dimensions $6 \times 6 \times 4.4$ mm with a diffusion rate of $5.6E-11$ m²/s led to an incubation time of approximately 3.5 h before significant changes in fluorescence could be observed.

CONCLUSION

The loss of fluorescence in cryogenically-treated cells and tissues is due to the diffusion of GFP from the cell/tissue onto the surrounding media (extracellular space/medium), onset by the cryogenic insult.

The loss of GFP in cryoinjured tissues will not, however, be immediately apparent, as the diffusion required to show regions of damaged tissue may take

hours. The required incubation period for cryoinjured GFP tissues before checking viability will depend on all environmental factors which govern diffusion. Future studies may be dedicated to determining the incubation period required given a variety of research conditions in a variety of tissues. For the samples used in this study, an incubation period of approximately 3.5 h is sufficient to observe a significant drop in fluorescence ($>10\%$).

Provided the aforementioned precautions and allowances are made, GFP may be successfully used as an indicator of viability in *ex vivo* GFP-transfected cryoinjured tissues. It shares all the same benefits of using GFP as a viability assay in single cells, while only requiring more time to exhibit and obtain the results. As fluorescence can be ascertained *in situ*, GFP as an indicator of viability in cryoinjured tissues can potentially be a valuable technique where more traditional assays may be inappropriate in preclinical trials.

ACKNOWLEDGMENTS

ABS acknowledges financial support from 2011 UC MEXUS Dissertation Research Grant.

CONFLICTS OF INTEREST

No conflicts of interest to declare.

REFERENCES

- ¹Alkaabi, K. M., A. Yafea, and S. S. Ashraf. Effect of pH on Thermal-and Chemical-Induced Denaturation of GFP. Heidelberg: Springer, 2005.
- ²Campbell, T. N., and F. Y. M. Choy. The effect of pH on green fluorescent protein: a brief review. *Mol. Biol. Today* 2(1):1-4, 2001.
- ³Elliott, G., J. McGrath, and E. Crockett-Torabi. Green fluorescent prote: a novel viability assay for cryobiological applications. *Cryobiology* 40(4):360-369, 2000.
- ⁴Ericsson, M., D. Hanstorp, P. Hagberg, J. Enger, and T. Nystrom. Sorting out bacterial viability with optical tweezers. *J. Bacteriol.* 182(19):5551-5555, 2000.
- ⁵Houtsmuller, A. B. Fluorescence recovery after photobleaching: application to nuclear proteins. *Adv. Biochem. Eng. Biotechnol.* 95:177-199, 2005.
- ⁶Leiderman, P., D. Huppert, and N. Agmon. Transition in the temperature-dependence of GFP fluorescence: from proton wires to proton exit. *Biophys. J.* 90(3):1009-1018, 2006.
- ⁷Martínez-Suástegui, L., B. Duperray, F. Godinez, G. Guillen, A. Slade, and G. Aguilar. Laser-assisted cryosurgery in *ex vivo* mice hepatic tissue: viability assays using green fluorescent protein. *Ann. Biomed. Eng.* 39(2):636-648, 2011.

- ⁸Mobility of Molecules and Particles within the Cytoplasm of a Living Cell. [http://www.zeiss.de/C12567BE00472A5C/EmbedTitelIntern/Application_Cellular_Cytoplasm/\\$File/CELLMEASURE2.PDF](http://www.zeiss.de/C12567BE00472A5C/EmbedTitelIntern/Application_Cellular_Cytoplasm/$File/CELLMEASURE2.PDF).
- ⁹Muldrew, K., M. Hurtig, K. Novak, N. Schachar, and L. E. McGann. Localization of freezing injury in articular cartilage. *Cryobiology* 31(1):31–38, 1994.
- ¹⁰Nagy, A., A. Málnási-Csizmadia, B. Somogyi, and D. Lorinczy. Thermal stability of chemically denatured green fluorescent protein (GFP): a preliminary study. *Thermochim. Acta* 410(1–2):161–163, 2004.
- ¹¹Saito, N., M. Zhao, L. Li, E. Baranov, M. Yang, Y. Ohta, K. Katsuoka, S. Penman, and R. M. Hoffman. High efficiency genetic modification of hair follicles and growing hair shafts. *Proc. Natl. Acad. Sci.* 99(20):13120–13124, 2002.
- ¹²Schaefer, B. C., M. L. Schaefer, J. W. Kappler, P. Marrack, and R. M. Kedl. Observation of antigen-dependent CD8 + T-cell/dendritic cell interactions in vivo. *Cell. Immunol.* 214(2):110–122, 2001.
- ¹³Schreer, A., C. Tinson, J. P. Sherry, and K. Schirmer. Application of Alamar blue/5-carboxyfluorescein diacetate acetoxymethyl ester as a noninvasive cell viability assay in primary hepatocytes from rainbow trout. *Anal. Biochem.* 344(1):76–85, 2005.
- ¹⁴Strebel, A., T. Harr, F. Bachmann, M. Wernli, and P. Erb. Green fluorescent protein as a novel tool to measure apoptosis and necrosis. *Cytometry* 43(2):126–133, 2001.
- ¹⁵Swaminathan, R., C. P. Hoang, and A. S. Verkman. Photobleaching recovery and anisotropy decay of green fluorescent protein GFP-S65T in solution and cells: cytoplasmic viscosity probed by green fluorescent protein translational and rotational diffusion. *Biophys. J.* 72(4):1900–1907, 1997.
- ¹⁶Wachsmuth, M., W. Waldeck, and J. Langowski. Anomalous diffusion of fluorescent probes inside living cell nuclei investigated by spatially-resolved fluorescence correlation spectroscopy. *J. Mol. Biol.* 298(4):677–689, 2000.
- ¹⁷Yang, H., J. Acker, A. Chen, and L. McGann. In situ assessment of cell viability. *Cell Transplant* 7(5):443–451, 1998.
- ¹⁸Youvan, D. C., and M. E. Michel-Beyerle. Structure and fluorescence mechanism of GFP. *Nat. Biotechnol.* 14:1219–1220, 1996.